Hindawi
Advances in Materials Science and Engineering
Volume 2020, Article ID 4589281, 7 pages
https://doi.org/10.1155/2020/4589281

*Research Article*

# Prototype Steam Turbine for Solar Power Production

**Kawira Millien**

*Department of Physical Sciences, University of Embu, P.O. Box 6–60100, Embu, Kenya*

Correspondence should be addressed to Kawira Millien; kawira.millien@gmail.com

Received 13 April 2020; Revised 23 June 2020; Accepted 25 June 2020; Published 20 July 2020

Academic Editor: Stefano Sorace

Copyright © 2020 Kawira Millien. This is an open access article distributed under the Creative Commons Attribution License, which permits unrestricted use, distribution, and reproduction in any medium, provided the original work is properly cited.

Fabrication of a prototype direct drive steam turbine using locally available materials provides a means to supply power and process heat for off-grid areas, which are not accessible due to rugged terrain. The use of solar power technologies to provide clean power and heat will mitigate environmental pollution and global warming that are caused by combustion of fossil fuels and other carbon-based power sources. The energy density of fossil fuels is higher than that of nonconcentrated solar power, which makes them a better option compared to nonconcentrated solar power sources. The high cost of steam thermal turbines and the limited technical skills on utilization of local materials for steam turbine construction have hampered the realization of potential of producing both small- and large-scale power in Africa. The design of the single-stage blade wheel system solar thermal turbine was done using AutoCAD 2010. The blades were made from encapsulated rice husk particle boards, and the steam casing was made from 0.0015 galvanized black iron sheet. Compensation for more stages was done by sending the fluid exiting from the turbine into the solar collector for reheating. It was coupled to a single-phase generator and gearbox. The rotor was made of galvanized iron tube. The turbine's average efficiency was obtained as 61.6% and average isentropic efficiency was 55.3%. The combined gearbox and generator approximate efficiency was 54.7%. Locally available heat transfer fluids were used for solar thermal collection. The prototype turbine was designed to produce 500 W of power. It had a heat rate ratio of 0.08. The turbine inlet conditions were as follows: average temperature of 112.8°C, average pressure of $2.7 \times 10^5\,\mathrm{Nm}^{-2}$, average enthalpy of 3156 kJ/kg, and average steam flow rate of 243.3 kg/hr. Outlet conditions were as follows: outlet average temperature of 97.3°C, average steam flow rate of 102.0 kg/hr, average pressure of $1.20 \times 10^5\,\mathrm{Nm}^{-2}$, and enthalpy of 2103 kJ/kg. With use of 6 M sodium chloride solution, the turbine inlet conditions were as follows: enthalpy of 3789.1 kJ/kg at a pressure of $3.0 \times 10^5\,\mathrm{Nm}^{-2}$ and its enthalpy at exit was 2346.3 kJ/kg at a pressure of $1.05 \times 10^5\,\mathrm{m}^{-2}$ which can provide process heat and power for off-grid areas.

## 1. Introduction

Adverse climatic change and environmental pollution are among the key issues of international interest due to the products of combustion from fossil energy resources and biomass-based materials, which cause global warming and pollution. Renewable energy technologies hold the solutions in mitigation of environmental pollution and climatic change, since they are of great significance in alleviating the pollution and climate change crisis.

Due to concerted industrialization endeavors, especially by developing countries, the demand for power in the world, in fact, is overwhelming. The energy demand, which has been increasing continuously throughout the years, is making development of renewable power technologies to be a necessity rather than an option, which indeed has been pushing towards depletion of the fossil fuels. Presently, renewable energy accounts for 18.2% of global energy consumption while the remaining 79.5% is obtained from oil, gas, and coal and 2.2% being produced from nuclear energy [1]. Specifically, in comparison with typical SEGS, solar plants that employ PTCs are well recognized and the technology is promising [2]. The greenhouse gases such as carbon (IV) oxide and carbon (II) oxide produced during combustion of the said materials increase the global temperature, making development of concentrated solar power and the paradigm change from conventional carbon-based fuels to renewable energy sources a stringent necessity. In addition to combustion, Jackson et al. [3] found that fossil fuel burning together with cement manufacturing release

about 90% of all carbon (IV) oxide emissions from human activities. Decarbonization via solar energy was predicted as the only major way to deal with the environmental and economic challenges caused by climate change [4]. The energy demand increases with increasing world population, and nowadays, the renewable energy technologies can provide process heat besides providing power. The enhanced demand for clean power and decarbonization has further exacerbated the energy security problem [5]. The economic, environmental, and safety factors are considered in deciding the type of energy source for utilization to produce power and process heat, considering the diverse needs of policy direction, which depends on whether a country has prioritized manufacturing industries and products processing or not. According to Kalogirou [6], among alternative energy sources, solar energy investment needs to be prioritized even though the initial cost of installation is higher. In terms of economic viability, established that solar energy systems provide electricity that is much cheaper than conventional energy supplied from fossil fuels and biomass besides the solar energy not emitting pollutants which are produced by the latter. In ordinary circumstances, carbon-based energy sources such as coal are preferred and more appealing, compared to nonconcentrated solar sources due to their higher energy densities, making them to be used more often for power production using boilers. However, research on renewable energy reveals that solar power is the most favorable resource [7] where an analytic hierarchy process model was studied. Besides, recent research has established that power production by use of screw expander technology can produce good efficiency at low to medium heat source temperatures [2]. In this study, 12.6% and 17.8% of maximum solar thermal power efficiency and exergetic efficiencies, respectively, were obtained. The screw expander technology consists of a rotary type positive displacement device which is characterized by absence of high-velocity working fluids, yet it is efficient enough to meet power demand. Back pressure steam turbines can be used for producing process heat in addition to power generation. Mechanical energy from steam was used for moving a rotor which was coupled to stator in a magnetic field. Use of the back pressure steam turbines has an advantage of being upgradable to cogenerate power and process heat in industries with high process heat demand such as tea processing industries while on the other hand, they can produce power for extraction of minerals such as copper. In an effort to produce cost-effective energy, 900 MW steam turbine cycle for off-design operation, using flue gases, was used to produce steam that increased the efficiency of the power plant by a large margin [8]. Multiple stage steam turbines, which operate on the principle of Rankine cycle, ensures that the steam discharge releases most of the thermal power before exiting the turbine. A convectional, ideal Rankine cycle operates between pressure of 30 kPa and 6 MPa at inlet temperatures of about 550°C. During design of steam turbine, if the interblade phase angle is between −45° and +90°, stall flutter was recorded to have a probability of occurrence [9]. The ratio of actual power generated by a turbine to the power which would be generated by an ideal turbine corresponds to the thermodynamic efficiency. An increase in efficiency of a steam turbine by 1% for 500 MW capacity led to minimal carbon (IV) oxide gas emissions to the environment [10]. To generate industrial power, multistage steam turbines are used to meet the demand, since the steam expansion takes place at all the stages, resulting in large energy conversion. However, steam turbines are not as competitive as screw expanders when the net power demand is smaller than 2 MW and for low grade heat sources [11]. A study showed that steam turbines produce about 90% of all electrical power used in United States of America [12]. In a study of solar systems, the input to any solar system was established to comprise of exergy [13]. The solar power intensity, which varies with time of day, determines the power output from solar power conversion technology device, and nowadays, renewable energy sources are characterized by low temperatures and low heat values, which have attracted increasing interest owing to their high accessibility amounts for exploitation. Process heat has much demand in industries such as agricultural produce processing, where materials produced are processed. In India, 70% of energy in form of thermal energy is used for applications below 250°C. A study on determination of environmental pollution from sea vessels traffic, by assessment of production and scattering of exhaust emitted by ships, when in manoeuvring mode and when in switching mode from heavy sulphur residual fuel to low sulphur distillate fuel oil, in the interest of mitigating sea environment pollution, creates interest in reducing pollution in the sea [14]. In this study, the fraction of sulphur (IV) oxide gas pollutant emission due to port activities of Naples city is nearly 40% which is substantial. In this regard, renewable energy technologies become necessary for pollution and climate change mitigation.

## 2. Materials and Methods

*2.1. Turbine Fabrication.* The means of fabrication of turbine was carried out by use of design guidelines by Jawad [15]. In this study, a single casing unit was fabricated using 2 mm thick galvanized black sheets. The rotor was coupled to a generator and gear box. It was fabricated using 1.5 mm thick galvanized iron tube. The solar thermal collector and heat exchanger were designed, fabricated, and tested [16,17].

The following factors were used in blade design: blade material, centrifugal bending stress, and load and dynamic pressure. The blade strength and vibration characteristics were tested using the blade trip timing process [18]. The fabricated turbine was a direct drive turbine with a single-stage blade wheel system as shown in Figure 1. The turbine blades were synthesized from rice husks and cassava adhesive particle board which were encapsulated with 2 mm aluminium casing [19]. The particle boards were synthesized in a study on synthesis of particle boards without use of harmful formaldehyde chemical [20]. The blades produced from the particle board had the following dimensions: 0.015 m thickness, radius of 0.02 m, 0.8 kg weight, and 0.7 m length. The steam was expanded in a nozzle inside the

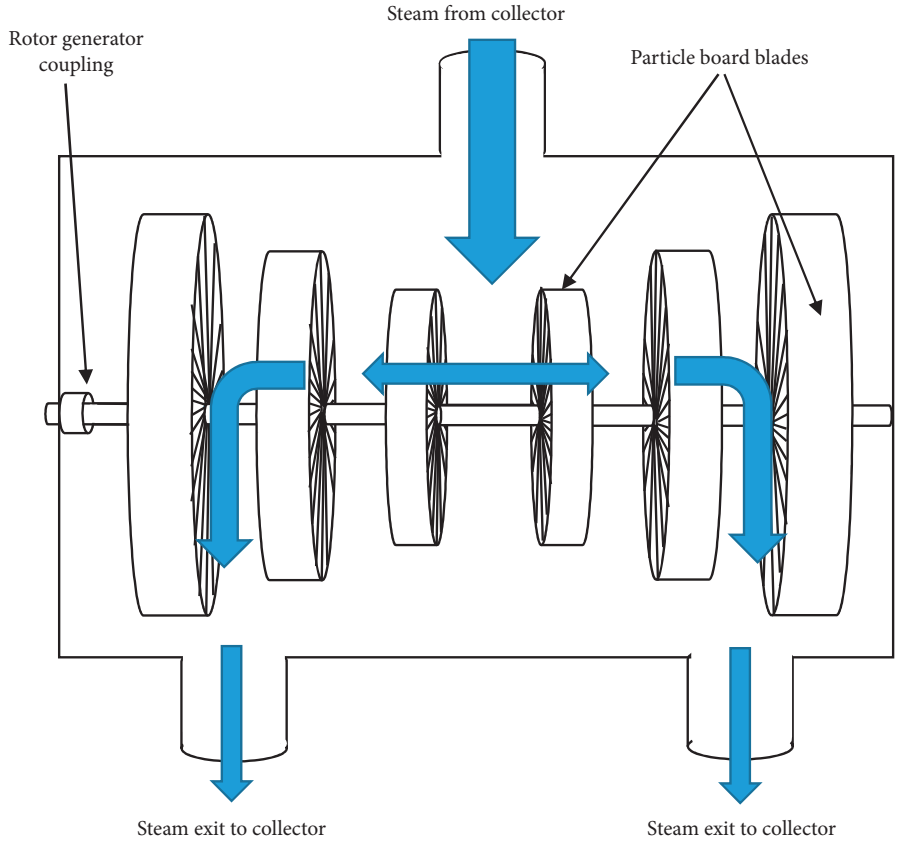


Figure 1: Single-stage blade system of the back pressure steam turbine.

turbine. Euler's turbine equation which is shown in equation (1) was used in the blade design [21].

$$V = h_{1+} + \frac{V_1^2}{2g} - h_2 - \frac{V_2^2}{2g} - \frac{U}{g}\left(W_{\theta 1} - W_{\theta 2}\right), \quad (1)$$

where $h_1$ and $h_2$ are the enthalpies of steam at entrance and exit, respectively, $V_1$ and $V_2$ are tangential absolute velocity components of fluid at inlet and exit, respectively, $W$ is relative velocity, $U$ is internal energy, and $g$ denotes the state of the fluid. The design layout was made by using AutoCAD 2010. The turbine bearings were of diameter of up to 340 mm with $L/D$ ratios of 0.4 to 0.21. Thrush bearings were used for shaft bearings. The turbine was designed to produce a rotor speed of 2800 rpm. It was machined to make provisions for contours and connection parts. Each end had a bearing, seal for gland, and a coupling area. Machining of axial grooves for the blades was made on the rotor. The steam turbine was connected to a single gear box coupled to a single-phase generator. In the study conducted by Zachos et al. [22], the finite element method was used for the structural design of the blade. Static analysis and thermal analysis were used during the blade design. The blades were fabricated individually and attached to the wheel disc. The moving blade tips were connected to a cover band which acted as a labyrinth that was fabricated, and it braced the moving blades to reduce the vibrations. The radial clearance was 0.3 m. The rotor was balanced both statically and dynamically after assembly of the blades. The rotor balancing was done at a low speed of 500 rpm with weight adjustments made in two planes, one at each end of the rotor. Provision was made to vary screwed plugs in tapped holes. Four pedestals were fabricated from galvanized iron rods of 1 mm diameter and 0.3 m length. They supported the turbine via the bearings in a fixed axial relationship.

Each blade was balanced individually before assembly. In the static balancing, the weight was displaced parallel to rotor axis until the blade balanced. In this study, the mass axis did not coincide with the rotational axis during the dynamic balancing. The balance was achieved by cutting away or addition of material from the rotor. Drilling, milling, and addition of material were done by bolting and welding of the balance weights at various points to achieve balance. The rotor was tested at speeds ranging from 500 rpm to 3000 rpm.

The galvanized iron tube rotor was of good creep resistance and withstood high temperature and had high fracture toughness. The bores of bearings were elliptical to provide geometry for hydrodynamic lubrication. Circular bores were machined with shims in horizontal split. Only one shaft bearing was used on the shaft line. During operation, oil was poured manually into the bearing via lead-in ports at two diametrically opposite points on the horizontal center line.

The rotating component consisted of a solid single-piece integrally forged rotor with hydrodynamic tilting pad bearings and flexible element couplings. The rotor had an

overlay welding of the batter passes and the final overlay welds were done using the SAW process [23]. The nozzle end diameter was 0.001 m such that the flow of steam through the nozzle was an adiabatic expansion. A control valve was threaded to the nozzle to control steam flow into the turbine. The nozzles were fabricated such that the cross section varied from 0.008 m to 0.001 m, and they were put at an angle of 30° to the blade. The angle used compared well with US Patent number US 3452132 [24].

Instead of using stages, the fluid exiting from the turbine was fed back into the turbine after reheating through the solar heat collector. The rotor design depended on the flow path and the size of inlet which was 0.001 m. The half pieces were bolted together, and rubber seals were put in between the half cases to prevent leakage of steam from the steam chamber. The generator bearings had $L/D$ ratios of 0.45 to 1.82.

The turbine efficiency $\eta$ was tested using different heat transfer fluids and was determined using equation (3) [25].

*2.2. Turbine Performance Characteristics.* The following performance characteristics of the turbine were determined: turbine isentropic efficiency (using equation (4)), steam flow rate (kg/hr), inlet pressure ($Nm^{-2}$), outlet pressure ($Nm^{-2}$), inlet temperature (°C), outlet temperature (°C), and net heat rate (J/W). The generator/gear box used had an efficiency of 54.7%.

The proportion of flash steam, $S_f$, was determined by setting the charging pressure by use of pressure control valve, and the discharge pressure was measured using the pressure gauge. Equation (2) was used to calculate the proportion of flash steam ($S_f$) with use of steam tables [26].

$$S_f = \frac{\left(h_{f1}(P_1)\right) - \left(h_{f2}(P_2)\right)}{h_{fg2}(P_2)}, \tag{2}$$

where $h_{f1}$ is the specific enthalpy of saturated water at inlet, $h_{f2}$ is the specific enthalpy of saturated water at outlet, and $h_{fg2}$ is the latent heat of saturated steam at outlet at respective pressures and temperatures. Steam tables (superheated and saturated) were used in the determination of the proportion of flash steam. The heat coefficients of steam at various temperatures were obtained from steam tables [27].

The efficiency, $\eta_{\text{th}}$ in equation 3, with respect to enthalpy of the heat transfer fluids, is each at a time and at different conditions of pressure and temperature, where $H_{\text{out}}$ is the output enthalpy of the heat transfer fluid and $H_{\text{in}}$ is the input enthalpy of the heat transfer fluid expressed as a percentage:

$$n_{\text{th}} = 1 - \frac{\left|H_{\text{out}}\right|}{\left|H_{\text{in}}\right|}, \tag{3}$$

where $H_{\text{in}}$ and $H_{\text{out}}$ are the enthalpy input and output, respectively.

The isentropic efficiency of the steam turbine was obtained using

$$\eta_T = \frac{H_1 - H_2}{H_1 - H_2^*}, \tag{4}$$

where $H_1$ is the enthalpy of high pressure inlet steam, $H_2$ is the actual enthalpy of exhaust low pressure steam, and $H_2^*$ is the pressure of the exhaust low pressure steam assuming isentropic expansion. The magnitudes of enthalpy were obtained by use of saturated and superheated steam tables with respect to pressures and temperatures of operation.

Energy input $\dot{E}_i$ was determined using equation (5) which is a product of mass flow rate of steam, $\dot{m}_i$, and the enthalpy at entry, $\dot{h}_i$ , of the steam [28]:

$$\dot{E}_i = \dot{m}_i \times \dot{h}_i. \tag{5}$$

The energy output $\dot{E}_o$ was determined by use of the product of mass flow rate of steam at exit, $\dot{m}_o$, and the enthalpy at exit, $\dot{h}_0$, as shown in the following equation [28]:

$$\dot{E}_o = \dot{m}_o \times \dot{h}_o. \tag{6}$$

The heat rate of the steam turbine was determined as a ratio of the net heat input and the turbine power as shown in the following equation:

$$\text{heat rate} = \frac{\text{heat input}}{\text{turbine power}}. \tag{7}$$

*2.3. Heat Transfer Fluid Performance.* The heat transfer fluids, namely, 6 M sodium chloride solution, 4 m sodium chloride solution, 2 M sodium chloride solution, unused engine oil, used engine oil, vegetable oil 2, and vegetable oil 1, were passed through a parabolic trough solar concentrator and then into heat exchanger with water as the secondary fluid [16,17]. The fabricated back pressure steam turbine was used for producing process steam and power. The steam from the collector via the heat exchanger was fed into the turbine input pipe where it expanded at the blades and exited at the outlet pipe. The temperature was measured using thermocouple sensors fixed at the inlet and the output of the steam turbine. Pressure was measured using steam pressure gauges with probes inside the inlet and outlet pipes of the steam turbine. The steam flow rate was measured using digital mass flow rate meters fixed at the inlet and outlet of the steam turbine. The enthalpy of the steam entering and leaving the steam turbine was determined using the superheated and saturated steam tables. The solar power intensity was measured using the solar power meter. The temperature of the heat transfer fluids was measured before and after exiting the solar collector. The secondary fluid which was water conducted solar thermal heat from heat transfer fluids. The heat exchanger was used to produce the steam which was fed into the turbine.

## 3. Results and Discussion

*3.1. Steam Turbine Characteristics.* The performance characteristics of the fabricated turbine were as follows: average isentropic efficiency of 55.3%, average cycle power output of 450.8 W, maximum power output of 498.2 W, generator/gear box efficiency of 54.7%, power/heat ratio of 0.08, inlet pressure of $3.60 \times 10^5\,Nm^{-2}$ to $2.5 \times 10^5\,Nm^{-2}$, average inlet temperature of 112.8°C, average outlet temperature of

Table 1: Average turbine efficiency for respective heat transfer fluids.

| Heat transfer fluid | Average turbine efficiency (%) |
|---|---|
| 6 M sodium chloride solution | 61.5 |
| 4 M sodium chloride solution | 61.05 |
| 2 M sodium chloride solution | 58.6 |
| Water | 54.8 |
| Unused engine oil | 53.5 |
| Used engine oil | 49.6 |
| Vegetable oil 2 | 47.5 |
| Vegetable oil 1 | 41.15 |

Table 2: Inlet and outlet enthalpies of heat transfer fluids.

| Heat transfer fluid | Enthalpy at inlet (kJ/kg) | Enthalpy at exit (kJ/kg) |
|---|---|---|
| 4 M sodium chloride solution | 3527.6 | 2211.3 |
| 2 M sodium chloride solution | 3456.3 | 2176.1 |
| Unused engine oil | 3377.4 | 2099.7 |
| Used engine oil | 30301.7 | 1812.4 |
| Vegetable oil 2 | 27548.2 | 16921.3 |
| Vegetable oil 1 | 2404.6 | 13,875.6 |

98.8°C, average inlet steam flow rate of 239.6 kg/hr, average outlet pressure of $1.20 \times 10^5\,\mathrm{Nm}^{-2}$ to $1.087 \times 10^5\,\mathrm{Nm}^{-2}$, and average outlet steam flow rate of 102 kg/hr.

In a study of AC generators, the torque was converted to power with efficiency higher than 90% [29]. The efficiency was higher than the one recorded in this study due to the better conductivity nature of the heat transfer fluid used. In addition, the efficiency in this study was lower due to the variations in the solar power intensity during the solar thermal collection.

The screw expander device achieved a high efficiency of 75%, where a couple of twin helical screw rotors, male and female rotors, are fixed on the parallel axis and bound to the case [2], compared to other steam conversion devices. This was also the case in this study, where the efficiency was lower due to the difference in the technologies used.

Table 1 shows the average efficiencies of the turbine with respect to the heat transfer fluids. The differences observed on the efficiencies tabulated are due to the variances of the solar thermal heat conducted by the fluids as they, respectively, flowed through the solar collector [17]. The salt solutions conducted more solar thermal heat compared to vegetable oil fluids and the engine oils lay in between. The unused engine oil conducted more heat compared to the used engine oil. Hence, the efficiencies of the heat transfer fluids ranged from 61.5% to 41.15%.

In US patent number US 3452132 A, 300°C of superheated steam and a manifold pressure of magnitude of $1.0 \times 10^{10}\,\mathrm{Nm}^{-2}$ were impinged asymmetrically on the yarn at an angle of 30°C, which was the angle that produced the highest power [30]; this was in order to produce industrial heat. In the endeavor to improve performance of steam turbine, it was established that to meet industrial power demand, a high speed turbine of 45000 rpm and a small blade span of length $200 \times 10^{-6}$ m would be required for optimum efficiency [31]. In this study, process heat and power were cogenerated.

*3.2. Turbine Performance with Heat Transfer Fluids.* The average enthalpy at inlet of the 6 M sodium chloride solution was 3789.1 kJ/kg at a pressure of $3.01 \times 10^5\,\mathrm{Nm}^{-2}$, and the enthalpy at exit was 2346.3 kJ/kg at a pressure of $1.05 \times 10^5\,\mathrm{Nm}^{-2}$. Table 2 shows the inlet and outlet enthalpies of the other heat transfer fluids under the same conditions as the 6 M sodium chloride solution.

Turbine efficiency was found to range from 65% for small turbines to 90% for bigger commercial ones [32]. In this study, the highest temperature of steam entering the turbine was an average of 120°C and the temperature of the fluid leaving the turbine was 98.0°C for an average output of 487 W.

Figure 2 shows the variation of steam flow rate and power output for the heat transfer fluids at an average solar power intensity of $1103.8\,\mathrm{Wm}^{-2}$. At 479 W, 6 M sodium chloride solution produced 298 kg/hr of steam at a temperature of 112 C and at a pressure of $1.24 \times 10^5\,\mathrm{Nm}^{-2}$. Vegetable oil 1 produced power of 336.3 W which produced steam flow rate of 68.9 kg/hr at a temperature of 97.5°C and a pressure of $1.04 \times 10^5\,\mathrm{Nm}^{-2}$. The steam flow rate was higher for the sodium chloride solutions while it was lower for vegetable oils as shown in Figure 2. This was because the vegetable oils absorbed less solar heat as they passed through the collector compared to the inorganic salt solutions and the engine oils. The unused engine oil produced higher steam flow rate compared to the used engine oil. This was because the used engine contained impurities, hence the lower steam flow rate. The performance of the engine oils lay in between the performance of the salt solutions and the vegetable oils. The mass flow rate of the secondary heat transfer fluid increased with the intensity of solar power

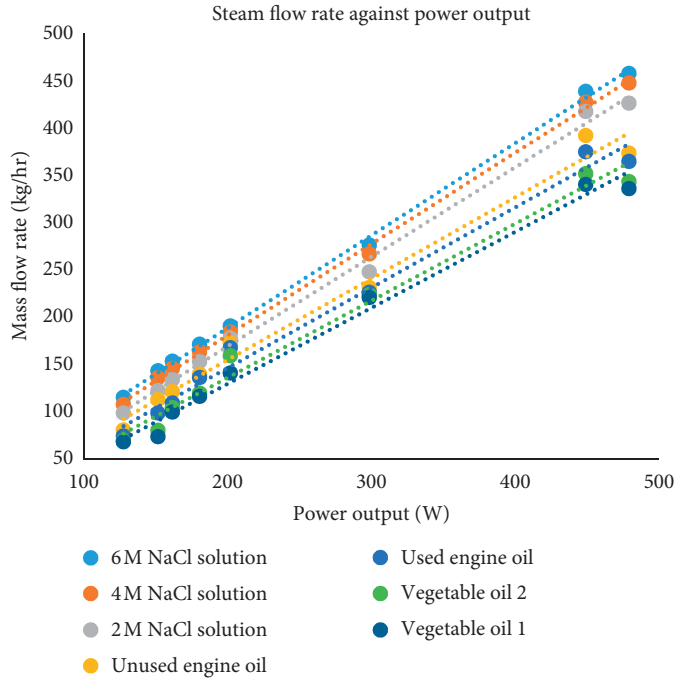


Figure 2: Steam turbine steam flow rate against power output for heat transfer fluids.

intensity. The measurement of power output and respective average steam flow rates were determined at an average solar power intensity of 1103.8 $Wm^{-2}$. In this study, the rotor was rotating at 2800 rpm which compared well with a rotor in a study which was carried out by Misek and Kubin [33] which rotated at 3000 rpm.

It was found that the generator must rotate at constant synchronous speed which is in tandem with the frequency of the power source [34] which was in tandem with the findings in this study.

## 4. Conclusion

Steam turbines, utilizing the power from the sun, can provide process heat and electrical power in off-grid areas, which are inaccessible due to rugged terrain. Local technology and materials have the potential of sustainability and in fact can be utilized for improving the energy demand locally. However, the heat transfer fluids need to be fortified against degradation to reduce the cost of production of the process heat and power. The steam that was exiting from the turbine at temperatures of an average of 109.0°C was used to heat the feed water, flowing into the absorber in the collector, and it was reheated by the collector before reentry into the turbine. The highest efficiency of the turbine was 61.6%, with respect to the 6 M sodium chloride solution, which achieved the highest enthalpy. The turbine operation conditions show that the turbine in this study can be upgraded to produce small scale industrial power and process heat. Improvement of temperatures of operation of the heat transfers fluids so that they degrade at higher temperatures and can lead to higher process heat and power production. In addition, increasing the thermal conductivity of the heat transfer fluids would increase the inlet steam enthalpy leading to increased process heat and power available for various industrial uses. The stepped up output can be used to run a medium industrial plant such as a fruits processing factory and mineral extraction industry.

## Nomenclature

$\dot{m}$: Mass flow rate (kg/h)
$\eta_{th}$: Efficiency with respective to enthalpy, %
$\eta_T$: Isentropic efficiency, %
$\dot{E}$: Energy flow rate (J/s)
$\dot{h}_i$: Enthalpy flow rate (J/kg)

*Abbreviations*

rpm: Rotations per minute
$L/D$: Length to diameter ratio
SAW: Submerged arch welding
US: United States of America
NaCl: Sodium chloride solution
$W$: Relative velocity in velocity triangle
SEGSs: Solar thermal electricity generating systems

*Subscripts*

1 and 2: Inlet and outlet streams
$\theta_1$ and $\theta_2$: Inlet and outlet velocity triangle angles
$g$: Gas
$h$: Enthalpy
in: Inlet
out: Outlet
$f$: Flash
$U$: Internal energy
$V$: Tangential absolute velocity components.

## Data Availability

The data used to support the findings of the study are available from the corresponding author upon request.

## Conflicts of Interest

The author declares that there are no conflicts of interest.

## References


[1] G. Dolf, B. Francisco, S. Deger, D. Morgan, W. Nicholas, and G. Ricardo, "The role of renewable energy in the global energy," *Energy Strategy Reviews*, vol. 24, pp. 38–50, 2019.

[2] P. Iodice, G. Langella, and A. Amoresano, "Modeling and energetic-exergetic evaluation of a novel screw expander-based direct steam generation solar system," *Applied Thermal Engineering*, vol. 155, pp. 82–95, 2019.

[3] R. Jackson, C. LeQuere, M. Andrew et al., "Global energy growth is outpacing decarbonization," *Environmental Research Letters*, vol. 13, no. 12, Article ID 120401, 2018.

[4] M. Mohsin, A. Rasheed, H. Sun et al., "Developing low carbon economies: an aggregated composite index based on carbon emissions," *Sustainable Energy Technologies and Assessments*, vol. 35, pp. 365–374, 2019.

[5] A. A. M. H. Ai Asbahi, F. Gang, W. Iqbal, Q. Abass, M. Mohsin, and R. Iram, "Novel approach of principal component analysis method to assess the national energy performance via energy trilemma index," *Energy Reports*, vol. 5, pp. 704–713, 2019.

[6] S. A. Kalogirou, "Solar thermal collectors and applications," *Progress in Energy and Combustion Science*, vol. 30, pp. 231–295, 2019.

[7] A. Salman and M. Razman, "Selection of renewable energy sources for sustainable development of electricity generation system using hierarchy process: a case study of Malaysia," *Journal of Renewable Energy*, vol. 63, pp. 458–466, 2014.

[8] M. Jaroslaw, B. Wojciech, W. Maran, F. Kamil, and K. Jan, "Off design operation of a 900 MW class power plant with utilization of low temperature of flue gases," 2015.

[9] Y. Zhang, K. Li, and D. Tao, "Effect of inter blade phase Angle on blade flutter of steam turbine," *Journal of Aerospace Power*, vol. 9, no. 3, p. 277, 1994.

[10] P. Subramanyam and K. Siva, "Experimental investigation on design of high pressure steam turbine blade," *International Journal of Innovative Research in Science, Engineering and Technology*, vol. 2, no. 5, 2013.

[11] P. Iodice, G. Langella, and A. Amoresano, "Energy performance and numerical optimization of a screw expander—based solar thermal electricity system in a wide range of fluctuating operating conditions," *International Journal of Energy Research*, vol. 44, no. 3, pp. 1858–1874, 2020.

[12] A. Chenduran, S. Tharani, G. Chenthooran, and S. Johnson, "Design of the steam turbine for small scale power plant," in *Proceedings of the Fifth Conference Proceedings, Department of Mechanical Engineering*University of Peradeniya, Sri Lanka, 2004.

[13] S. A. Kalogirou, S. Karellas, K. Braimakis, C. Stanciu, and V. Badescu, "Exergy analysis of solar thermal collectors and processes," *Progress in Energy and Combustion Science*, vol. 56, pp. 106–137, 2016.

[14] P. Iodice, G. Langella, and A. Amoresano, "A numerical approach to assess air pollution by ship engines in manoeuvring mode and fuel switch conditions," *Energy & Environment*, vol. 28, no. 8, pp. 827–845, 2017.

[15] M. H. Jawad, *Theory and Design of Plate and Shell Structures*, Chapman and Hall Publishing Ltd, New York, NY, USA, 1994.

[16] M. Kawira, R. Kinyua, and J. Kamau, "A prototype steam storage system for power production," *International Journal of Scientific Engineering and Technology (IJSET)*, vol. 3, no. 8, pp. 1012–1015, 2014.

[17] M. Kawira, R. Kinyua, and J. Kamau, "A prototype parabolic trough solar concentrator for steam production," *Journal of Agriculture Science and Technology (JAGST)*, vol. 14, no. 2, 2012.

[18] G. Janick and M. Byron, "Turbine blade vibration measurement methods for turbocharges," *American Journal of Sensor Technology*, vol. 2, no. 2, pp. 13–19, 2014.

[19] S. W. Kariuki, J. Wachira, M. Kawira, and G. M. Leonard, "Characterization of prototype formulated particleboards from agro industrial lignocellulose biomass bonded with chemically modified cassava peel starch," *Advances in Materials Science and Engineering*, vol. 2019, Article ID 1615629, 15 pages, 2019.

[20] S. W. Kariuki, J. Wachira, M. Kawira, and G. M. Murithi, "Formaldehyde use and alternative biobased binders for particleboard formulation: a Review," *Journal of Chemistry*, vol. 2019, Article ID 5256897, 12 pages, 2019.

[21] W. B. Jechens, "Steam turbines—their construction, selection and operation," in *Proceedings of the South African Sugar Technologies Association*, Durban, South Africa, March 1966.

[22] P. K. Zachos, M. Pappa, and A. I. Kalfas, "Turbine blading performance evaluation using geometry scanning and flow prediction tools," *Journal of Power and Energy Systems*, vol. 2, no. 6, pp. 1345–1358, 2008.

[23] K. Weman, *Welding Process Handbook*, Elsevier, Science Direct, Amsterdam, Netherlands, 2nd edition, 2012.

[24] G. Pitzl: Process of steam drawing and annealing polyester yarn, US Patent US3452132A, 1969.

[25] M. Eck, E. Zarza, M. Eickhoff, J. Rheinländer, and L. Valenzuela, "Applied research concerning the direct steam generation in parabolic troughs," *Solar Energy*, vol. 74, no. 4, pp. 341–351, 2003.

[26] E. F. Church, *Steam Turbines*, Mc Graw Hill Publishers Ltd., London, UK, 1987.

[27] C. H. Peabody, *Thermodynamics of the Steam Engine and Other Heat Engines*, Wiley and Sons Publishers Ltd., New York, NY, USA, 2011.

[28] A. H. Ranah and J. R. Mehta, "Energy and exergy analysis of extraction cum back pressure steam turbine," *Journal of Modern Engineering Research*, vol. 3, no. 2, pp. 626–632, 2013.

[29] C. Whitaker, *AC Power Systems Handbook*, Taylor and Francis, Boca Raton, FL, USA, 2006.

[30] P. Gilbert, "Process of Steam drawing and annealing,"Assigned to Du Point, US Patent No. US 3452132 A, Assigned to Du Point, pp. 1593–1658, Atlanta, Georgia, 1969.

[31] S. Satos, S. Jovanovic, J. Lang, and Z. Spakovscky, "Demonstration of a palm sized 30 W air-to-power turbine generator," *Journal of Engineering for Gas Turbines and Power*, vol. 133, no. 10, pp. 1–10, 2011.

[32] A. Schetz and A. E. Fuhs, *Hand Book of Fluid Dynamics and Fluid Machinery*, Oxford Press, New York, NY, USA, 1996.

[33] T. Misek and Z. Kubin, "Static and dynamic analysis 0f 1220 mm steel last stage blade for steam turbine," in *Proceedings of the Applied and Computational Mechanics Symposium*, pp. 133–140, Honolulu, Hawaii, March 2009.

[34] A. Leyzerovich, *Wet Steam Turbines for Nuclear Power Plants*, Pen Well Books, Tusla, Oklahoma, 2005.